EVS27
Barcelona, Spain, November 17-20, 2013

Predictive Real-Time Energy Management Strategy for PHEV using Lookup-Table-based Dynamic Programming

B. Bader[1], O. Torres[1], J.A. Ortega[1], G. Lux[2], J.L. Romeral[1,3]
[1]*MCIA, Department of Electronic Engineering, Technical University of Catalonia (UPC), Spain*
[2]*SEAT Technical Centre, Spain* [3]*CTM Technical Centre, Spain*

Abstract

This paper proposes a predictive real time energy management strategy for plug-in- hybrid electric vehicles (PHEV) based on an adaptation of Dynamic Programming (DP). The computational load of predictive real time strategies increases with the trip length. Therefore, for online computation by the onboard computer, they strongly depend on an efficient implementation. To reduce computation cost, current approaches for predictive strategies rely on strongly simplified intern vehicle models. The here proposed energy management strategy (EMS) uses a different approach, which is based on the use of precalculated lookup tables for the different operating points of the powertrain. This precalculation make the use of more exact vehicle models possible by using more detailed loss models of the powertrain components. The proposed EMS separates the optimization process, i.e. the calculation of the power distribution to engine and electric motor and gear in two calculation steps. The first step, which is computationally more intensive, has only to be executed once for a certain vehicle configuration. The obtained results are saved in lookup tables to avoid a later recomputation. In the second step, which is done online in the vehicle, a shortest path search algorithm is employed which is based on the predicted vehicle speed and rode slope of the trip. Techniques are integrated which decrease the rounding error caused by the use of lookup tables. The resulting difference of the consumed fuel mass between the lookup table based DP and standard DP is smaller than 0.03% by an approximately 50 times faster calculation. Using the proposed algorithm, even complex intern vehicle models do not affect the online computation cost and can be implemented by real time strategies.

Keywords: HEV (hybrid electric vehicle), parallel HEV, PHEV (plug in hybrid electric vehicle), optimization, power management

1 Introduction

Environmental issues caused by the transportation sector green house gas emissions, as well as the risen oil prices, have lead to an increased demand for fuel saving vehicles. Among the measures to reduce fuel consumption are the use of lightweight materials, the downsizing of the combustion engine or the powertrain hybridization. Powertrain hybridization by the integration of an additional electric motor with energy strore, permits the combustion engine to operate in higher efficiency regions and therefore with a lower fuel consumption. In addition, part of the kinetic energy of the vehicle

can be regenerated by braking with the electric machine. PHEV offer in contrast to autonomous hybrid electric vehicles (HEV) not only a more efficient use of fuel, but in addition, they can substitute fuel energy by electric energy. By the use of electric energy it is possible to reduce the ecologic impact and the dependence of petrol of the transportation. Therefore, and because of the current battery capacity restrictions and high costs of the actual battery technology, PHEV are a compromise between pure electric and HEV. When used for typically daily trip distances e.g. from home to work, a major substitution of fuel energy by electric energy can be reached. In addition, the range of PHEV is not restricted by the battery capacity, as it is for pure electric vehicles. The use of both electric motor and engine in (P)HEV requires an EMS which controls the energy distribution to both machines at every instant. The EMS has an even stronger influence on the vehicle fuel consumption and energy efficiency.

As battery of a PHEV can be recharged at the trip end, the principal operation mode of PHEV is the charge depleting mode (CD). In the CD mode the stored electric energy is consumed until the end of the trip for minimal fuel consumption. This could be done by starting the trip in electric mode and switch at a low state of charge (SOC) to the charge sustaining mode (CS). More efficient is the use of a blended strategy, which employs the combustion engine from the beginning of the trip [1]. Therefore, especially for PHEV it is useful to employ predictive strategies, which use information about the power demand during the future trip until the next recharge of the battery. The information about the future trip can be obtained from prediction algorithms which combine the information from new generation navigation systems and knowledge of the driver's behavior by the use of Neural Networks [2].

The EMS controls the optimal combination of the gear, the torque of the internal combustion engine (ICE) T_{ice} and the electric machine torque T_{em}. A lot of EMS concepts have been studied [3] and can be classified into heuristic and optimization based strategies. Among the heuristic controllers are rule based systems [4] or fuzzy controller [5] [6]. Among the optimization based approaches is Pontryagin's Principle [7] [8], which has been used first for HEV [9], and later been adapted to the requirements of PHEV [10]. Another possible approach is DP [11] or the combination of both and a Pontryagin's Principle approach [12]. DP is due to its high computational effort normally used for benchmark purposes and can be used for real time EMS only employing high power and thus expensive onboard computer in the vehicle. Therefore, current predictive real time EMS employ faster optimization algorithms which are based on strongly simplified intern vehicle models to achieve low computation cost[13]. To avoid the online execution of DP, it is also used as Stochastic Dynamic Programming when stochastic cycle data is used for the optimization [14]. In [15] Quadratic Programming is used to optimize the future ratio of the torque between both machines and taking into account the energy of the battery. These strategies have in common that they optimize a model based on Willans lines for the engine and a corresponding approach for the electric motor [16]. If a speed dependent component is included in these models, it is only limited to rough approximation of the speed. A more exact optimization, i.e. getting results closer to the global optimum, is achieved by using fuel and loss tables for engine and electric motor. As for the use of fuel and efficiency tables the motor/engine speed has to be known, the complexity of the model is increased, what results in higher computation cost. To overcome this problem, a technique is presented which allows a significant reduction of the computation cost of DP when used in an EMS of a specific vehicle. The proposed EMS reduces computational effort by the beforehand calculated lookup tables. It is able to optimize the power distribution for the future trip and finds a solution close to the global optimum. The algorithm includes also the gear pattern in the optimization. It is assumed that vehicle speed and road grade is known to the EMS a priori.

In Section 2 of this paper, the employed models and simulation environments are presented. In Section 3 the EMS algorithm based on a DP approach is presented. The results of the validation are shown in Section 4.

2 Simulation Environment

2.1 Vehicle Structure

The simulated hybrid drivetrain has a parallel structure; the electric motor and the combustion engine are mounted on the same drive shaft. The ICE can be separated by a clutch from the powertrain for electric driving without the friction losses of the engine (Fig. 1). The double clutch gearbox has seven gears. Due to the double clutch

principle, fast gear shifting is assumed and shifting losses are not considered in the powertrain model. The body parameters are similar to a conventional SEAT Ibiza ST passenger car, taking into account the weight of the additional electric components as battery and electric motor. The battery has a capacity of 4kWh and can be recharged during the trip by the electric motor in generator mode or at the trip end by connecting it to the electric grid.

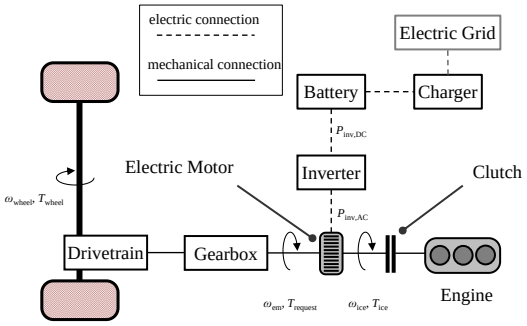

Fig. 1. Powertrain scheme of a parallel PHEV. The combustion engine can be separated from the drivetrain by a clutch. By connecting the charger to the electric grid the battery can be recharged.

Table I: Simulation Parameter

Symbol	Quantity	Value	Unit
m	vehicle mass	1450	kg
A_f	vehicle frontal area	2.2	m²
c_w	drag coefficient	0.325	-
μ_r	rolling resistance	0.01	-
r_{wheel}	wheel radius	0.29	m
$P_{\text{ice,max}}$	max. power ICE	51	kW
$T_{\text{ice,max}}$	max. torque ICE	110	Nm
$P_{\text{em,max}}$	max. power EM	80	kW
$T_{\text{em,max}}$	max. torque EM	400	Nm
$E_{\text{battery,nom}}$	battery capacity	4	kWh
V_0	battery voltage	300	V
R_{battery}	inner battery resistance	366.67	mΩ

2.2 Vehicle Model

The vehicle model is created in the simulation environment MODELICA/DYMOLA. Two different models are used; a backward model which is used by the DP algorithm, and a forward model in which the resulting EMS is simulated. In the following, the different model components are shortly described. The wheel force is calculated as a function of among others vehicle mass m, wheel inertia J_{wheel} and the horizontal angle of the road α (Table I) by

$$F_{\text{wheel}}(v,\alpha) = \mu_{\text{roll}} mg + (+\frac{J_{\text{wheel}}}{r_{\text{wheel}}^2})a + \frac{1}{2}\rho c_w A_f v^2 mg \sin(\alpha) \quad . \tag{1}$$

The wheel torque during the driving cycle is obtained using (1):

$$T_{\text{wheel}}(v,\alpha) = F_{\text{wheel}}(v,\alpha)\, r_{\text{wheel}} \quad . \tag{2}$$

Due to the parallel structure of the powertrain, the engine torque T_{ice} and the electric motor T_{em} are added up and yield the total torque which corresponds to the torque requested by the driver T_{request}:

$$T_{\text{request}} = T_{\text{em}} + T_{\text{ice}} \quad . \tag{3}$$

In the forward model the requested torque is controlled by a PI controller for the accelerator and brake pedal, adapting them depending on the difference between actual vehicle speed v and cycle speed v_{cycle}. In the backward model used by the DP algorithm, a driver model is omitted, assuming that the vehicle speed v corresponds at every instance exactly the driving cycle speed v_{cycle}. With (1), (2) and

$$P_{\text{wheel}}(v,\alpha) = T_{\text{wheel}}(v,\alpha)\, v \tag{4}$$

results that also the power P_{wheel} transferred from the wheels to the road corresponds in the backward model at every instance the power requirement of the cycle P_{cycle}.

$$P_{\text{cycle}} = P_{\text{wheel}}(v_{\text{cycle}}, \alpha_{\text{cycle}}) \quad . \tag{5}$$

The torque T_{request} stands in a direct relation with the wheel torque T_{wheel} as function of the driving cycle (see (2)) and of the gearbox efficiency η_{trans} and transmission ratio g_r (which includes both gearbox ratio and final drive):

$$T_{\text{request}} = \begin{cases} \frac{T_{\text{wheel}}}{\eta_{\text{trans}}\, g_r} & T_{\text{wheel}} > 0 \\ \frac{T_{\text{wheel}}\, \eta_{\text{trans}}}{g_r} & T_{\text{wheel}} \leq 0 \end{cases} \quad . \tag{6}$$

The speed of the electric motor depends on the cycle speed v_{cycle} and the transmission ratio g_r

$$\omega_{\mathrm{em}} = v_{\mathrm{cycle}}\ r_{\mathrm{wheel}}\ g_r \quad . \tag{7}$$

while the speed of the combustion engine corresponds to the speed of the electric motor when the clutch is closed, otherwise it is 0:

$$\omega_{\mathrm{ice}} = \begin{cases} 0 & \text{clutch open} \\ \omega_{\mathrm{em}} & \text{clutch closed} \end{cases} \quad . \tag{8}$$

2.2.1 Combustion Engine

The fuel consumption of the combustion engine is modeled by a measured consumption map of a 51kW engine. The calculated revolution number and the torque demand are used to interpolate the corresponding fuel consumption map as a function of engine torque T_{ice} and angular velocity of the engine shaft ω_{ice}

$$\dot{m}_{\mathrm{fuel}} = f_{\mathrm{fuel}}(T_{\mathrm{ice}}, \omega_{\mathrm{ice}}) \quad . \tag{9}$$

2.2.2 Electric Traction System

For the electric motor, the electric losses are modeled by an electric losses map. Similar to the combustion engine, electric motor speed ω_{em} and torque T_{em} are used determine the electric losses and thus the electric power input.

$$P_{\mathrm{inv,AC}} = \begin{cases} P_{\mathrm{mech}} + f_{\mathrm{losses}}(T_{\mathrm{em}}, \omega_{\mathrm{em}}) & P_{\mathrm{mech}} > 0 \\ P_{\mathrm{mech}} - f_{\mathrm{losses}}(T_{\mathrm{em}}, \omega_{\mathrm{em}}) & P_{\mathrm{mech}} \leq 0 \end{cases} \quad . \tag{10}$$

For the inverter a constant efficiency of 92% is assumed:

$$P_{\mathrm{inv,DC}} = \begin{cases} \frac{P_{\mathrm{inv,AC}}}{\eta_{\mathrm{inv}}} & P_{\mathrm{inv,AC}} > 0 \\ P_{\mathrm{inv,AC}}\eta_{\mathrm{inv}} & P_{\mathrm{inv,AC}} \leq 0 \end{cases} \quad . \tag{11}$$

The battery loss is modeled by the internal resistance R_i. Two different models are employed depending on whether the battery is charging ($P_{\mathrm{inv,DC}}$<0) or is supplying energy ($P_{\mathrm{batt}} \geq 0$). In the first case, i.e. $P_{\mathrm{inv,DC}} < 0$, P_{batt} is calculated in dependence of $P_{\mathrm{inv,DC}}$:

$$P_{\mathrm{batt}} = \frac{{V_0}^2 - V_0\sqrt{V_0^2 - 4P_{\mathrm{inv,DC}}R_i}}{2R_i} \quad . \tag{12}$$

In traction mode, when $P_{\mathrm{inv,DC}} \geq 0$,

$$P_{\mathrm{inv,DC}} = P_{\mathrm{batt}} - \left(\frac{P_{\mathrm{batt}}}{V_0}\right)^2 R_i \tag{13}$$

is used. The energy content of the battery is a function of the power P_{batt} delivered to the inverter.

$$E_{\mathrm{batt}}(t) = E_{\mathrm{batt}}(t_0) - \int_0^t P_{\mathrm{batt}}(t')dt' \quad . \tag{14}$$

The SOC is a function of the battery charge $Q(t)$ and the nominal battery charge Q_{nom}. With the open circuit voltage assumed to be constant, the SOC is equal to the ratio of the energy stored in the battery and the nominal energy capacity:

$$\mathrm{SOC} = \frac{Q_{\mathrm{batt}}}{Q_{\mathrm{batt,nom}}} = \frac{E_{\mathrm{batt}}}{E_{\mathrm{batt,nom}}} \quad . \tag{15}$$

2.3 Driving Cycle

To demonstrate the correct operation of the proposed algorithm, a recorded driving cycle from Barcelona to the company SEAT (called BCN-CTS, Fig. 2) is simulated. It describes a typical driving pattern of people working in a nearby city consisting of an urban part at the beginning and the end and a highway part in the middle. In this cycle also elevation information of the road is included. The characteristics are summarized in the table below (Table II).

Table II: Characteristics of the driving cycle BCN-CTS

duration	1903s	v_{max}	117.4km/h
length	33.1km	v_{avg}	62.6km/h
Δh	107.6m		

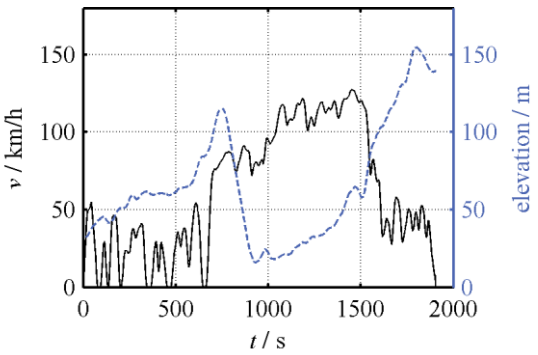

Fig. 2. Speed and elevation of the driving cycle BCN-CTS

3 Dynamic Programming

Dynamic Programming (DP) is a algorithm based on the optimality principle of Bellman [17] to calculate the global optimal solution of a discrete

stochastic or deterministic optimization task. As it is frequently used for the calculation of the optimal fuel consumption of HEV, the basics are only shortly described. The focus is put on the innovation of the proposed algorithm. As the optimization task is assumed to be deterministic, the resulting problem is a shortest path problem [18].

As the algorithm can be applied only on a discrete optimization problem, a discretization grid for the time and the states of the model has to be defined. A narrower grid results in higher accuracy but requires also more computation time. Due to the non-algebraic characteristic of the algorithm, the computation cost is high compared with algorithms like Quadratic Programming (QP) or Pontryagin's Principle. The computation cost of DP increases exponentially with the number of states (states arise usually from energy storages as inertias or the battery). To limit computation cost, only the SOC is used as only model state for the static backward model described above.

The system to which the optimization is applied can be generally be described by

$$x(k+1) = f_k\big(x(k), \vec{u}(k)\big) \quad , \quad (16)$$

where $x(k)$ is the state and $\vec{u}(k)$ the control variable at time step k. The function f_k stands for the vehicle model described above. The control variable $\vec{u}$ is the torque of the electric machine T_{em} and the gear g

$$\vec{u}(k) = \begin{bmatrix} T_{\mathrm{em}}(k) \\ g(k) \end{bmatrix} \quad . \quad (17)$$

Using these control variables the engine torque T_{ice} is defined with (3). With (16) results:

$$E_{\mathrm{batt}}(k+1) = f_k\big(E_{\mathrm{batt}}(k), u(k)\big) \quad . \quad (18)$$

The control problem can be formulated as finding the optimal control sequence

$$\begin{aligned}\left(\pi_i^{\mathrm{opt}}\right) &= (u(1), u(2), \dots u(N)) \\ &= \arg\min_{\pi\in\Pi} m_{\mathrm{fuel},\pi}(x_0)\end{aligned} \quad (19)$$

which minimizes

$$J^{\mathrm{opt}}(x_0) = \min_{\pi\in\Pi} m_{\mathrm{fuel},\pi}(x_0) \quad (20)$$

where Π is the set of all possible control sequences, and x_0 the system state at time step 0. Due to the discretization of the time, the cycle speed v, acceleration a and slope Δh can be expressed as sequences

$$\begin{aligned}(v_i) &= (v_1, v_2, \dots, v_n) \\ (a_i) &= (a_1, a_2, \dots, a_n) \\ (\Delta h_i) &= (\Delta h_1, \Delta h_2, \dots, \Delta h_n)\end{aligned} \quad (21)$$

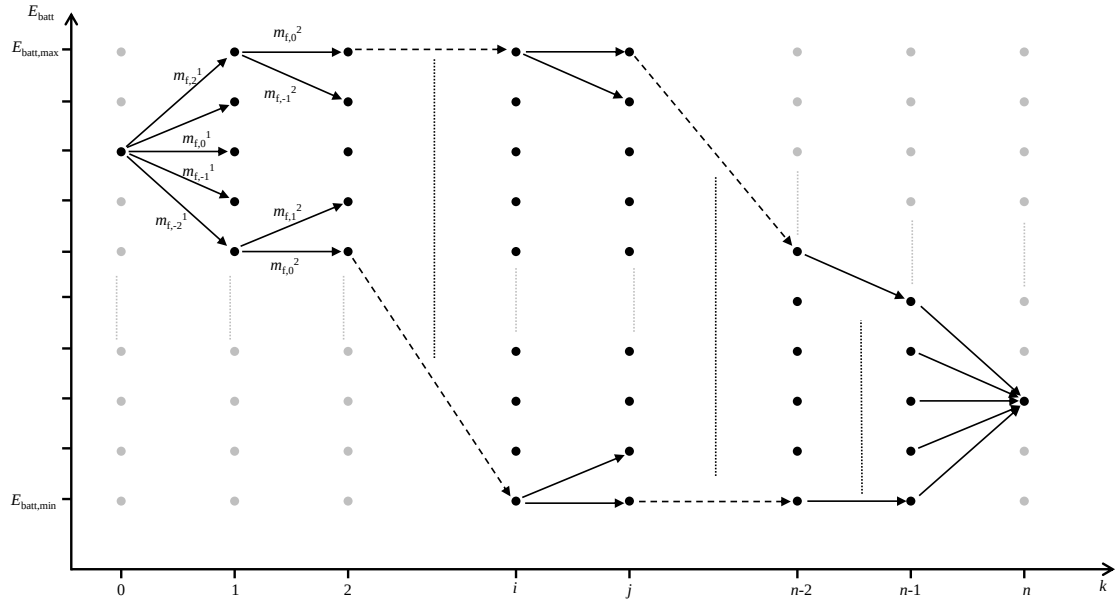

Fig. 3. DP best way search of a charge depleting strategy. The energy state of the battery E_{batt} is discretized over time and energy content. The algorithm searches the way which minimizes the cost function J_π.

3.1 Calculation of the Lookup Tables

To apply the best way search algorithm used by DP in (20), for the sequences in (21) the optimal gear is calculated by

$$g(k) = \underset{m_{\text{fuel}}}{\operatorname{argmin}} f_k(dE_{\text{batt}}, v_{\text{cycle}}, a_{\text{cycle}}, \Delta h_{\text{cycle}}, g) \quad (22)$$

and the fuel consumption $m_{\text{fuel}}(k)$ for every edge in Fig. 3 is calculated in function of the gear by

$$m_{\text{fuel}}(k) = \min_{g} f_k(\mathrm{d}E_{\text{batt}}, v_{\text{cycle}}, a_{\text{cycle}}, \Delta h_{\text{cycle}}, g(k)) \quad . \quad (23)$$

The value $\mathrm{d}E_{\text{batt}}$ describes the energy change of the battery during one time step. The value is a multiple of the grid spacing of 1kJ plus a displacement $E_{\text{batt,shift}}$:

$$\mathrm{d}E_{\text{batt}} = k \cdot 1\text{kJ} + E_{\text{batt,shift}} \quad k \in \mathbb{Z} \quad . \quad (24)$$

$E_{\text{batt,shift}}$ is chosen in a way that the energy change of the battery in pure electric mode can be described exactly by (24), that is

$$E_{\text{batt,shift}} = dE_{\text{batt,E-Mode}} - k_1 \cdot 1\text{kJ} \quad . \quad (25)$$

This decreases the effect of rounding errors caused by the grid width of 1kJ in electric mode [19], and thus making the best way search more exact. The corresponding torques T_{em} and T_{ice} can also be calculated for every edge as function of cycle and gear:

$$T_{\text{ice}} = g'''(\mathrm{d}E_{\text{batt}}, v_{\text{cycle}}, P_{\text{cycle}}, g)$$
$$T_{\text{em}} = g''''(\mathrm{d}E_{\text{batt}}, v_{\text{cycle}}, P_{\text{cycle}}, g) \quad . \quad (26)$$

As the weight m_{fuel} of each edge is a function of P_{cycle} and and v_{cyle} the value can be saved together with the corresponding value of gear g and engine and motor torque. To limit the entries of the lookup table, the power is saved in a spacing of 1kW giving the set

$$\frac{\{P_{\text{table}}\}}{\text{kW}} = \{-40, -39, \ldots, 0, \ldots, 40\} \quad (27)$$

and a speed spacing of 1km/h

$$\frac{\{v_{\text{table}}\}}{\text{km/h}} = \{0,1,2,\ldots,160\} \quad . \quad (28)$$

The resulting lookup table is a 3-dimensional array (Fig. 4). The resulting lookup tables have for the proposed grid defined in (27) and (28)

$$n_{\text{elements}} = 81 \cdot 161 \cdot 119 = 1551879 \quad (29)$$

elements. Considering that four tables are necessary for T_{ice}, T_{em}, the gear g and fuel mass m_{fuel} the above number has to be multiplied by factor four. By saving them in a single floating point format, a total lookup table size of about 24MB results.

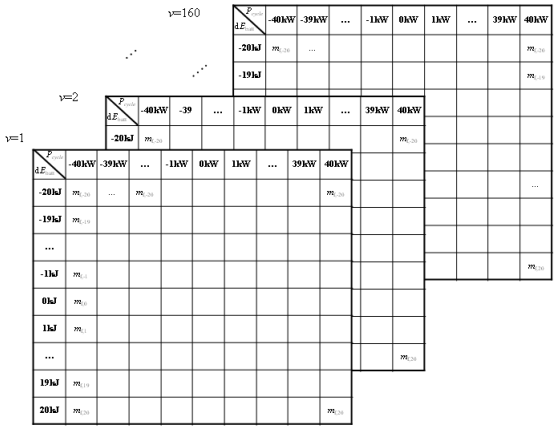

Fig. 4. Lookup tables for DP algorithm. The values for m_{fuel}, T_{ice}, T_{em} and gear have to be calculated once for a certain vehicle and are saved in these lookup tables. The values are saved for every combination of v_{cycle}, P_{cycle} and $\mathrm{d}E_{\text{batt}}$, thus resulting in a 3-dimensional array.

3.2 Application of the Lookup Tables

Using the known cycle data $v_{\text{cycle}}(k)$, $a_{\text{cycle}}(k)$, $\Delta h(k)$ in (1) the wheel force F_{wheel} can be calculated for the future trip. Beforehand, to minimize the problem of the time grid of 1s the velocity is averaged over the current and the next time point.

$$\bar{v}_{\text{cycle}}(k) = \frac{v_{\text{cycle}}(k) + v_{\text{cycle}}(k+1)}{2} \quad (30)$$

which is also done for the slope

$$\overline{\Delta h}_{\text{cycle}}(k) = \frac{\Delta h_{\text{cycle}}(k) + \Delta h_{\text{cycle}}(k+1)}{2} \quad . \quad (31)$$

By doing so, the change of speed v_{cycle} and slope during a time step is taken into account. The power at every instance can be calculated by

$$\bar{P}_{\text{cycle}}(k) = f_{F_{\text{wheel}}}(\bar{v}(k), \overline{\Delta h}(k), \text{a}(k))$$
$$\bar{P}_{\text{wheel}}(k) = F_{\text{wheel}}(\bar{v}(k), \overline{\Delta h}(k), \text{a}(k))\bar{v}_{\text{cycle}}(k) \quad (32)$$

yielding the sequence of the required power during the driving cycle

$$(P_{\text{wheel},i}) = (P_{\text{wheel},1}, P_{\text{wheel},2}, \dots, P_{\text{wheel},n}) \quad (33)$$

converted into the sequences (P_i), (v_i). When accessing the lookup tables, the values are rounded to the grid spacing of 1km/h and 1s.

$$v'_{\text{cycle}}(k) = \text{round}(\bar{v}_{\text{cycle}}(k))$$
$$P'_{\text{cycle}}(k) = \text{round}(\bar{P}_{\text{cycle}}(k)) \quad . \quad (34)$$

The corresponding values for T_{em}, T_{ice}, and $\dot{m}_{\text{fuel}}$ are taken from the corresponding lookup table $F_{m_{\text{fuel}}}$, $F_{T_{\text{ice}}}$.

$$\vec{m}_{\text{fuel}} = F_{m_f}(P'_{\text{cycle}}(k), v'_{\text{cycle}}(k))$$
$$\vec{t}_{\text{ice}}(k) = F_{T_{\text{ice}}}(P'_{\text{cycle}}(k), v'_{\text{cycle}}(k)) \quad . \quad (35)$$

The vectors $\vec{T}_{\text{em}}(k)$ and the displacement $E_{\text{shift}}(k)$ of (27) are also taken from the corresponding lookup tables $F_{T_{\text{em}}}$ and $F_{E_{\text{shift}}}$

$$\vec{t}_{\text{em}}(k) = F_{T_{\text{em}}}(P'_{\text{cycle}}(k), v'_{\text{cycle}}(k))$$
$$E_{\text{shift}}(k) = F_{E_{\text{shift}}}(P'_{\text{cycle}}(k), v'_{\text{cycle}}(k)) \quad (36)$$

and adapted by an estimation of the rounding error caused by the rounding of P'_{cycle}. To compensate these resulting rounding errors of torque and battery energy consumption, a compensation for T_{em} and the energy offset E_{shift} is calculated for every time step. Therefore, the rounding error of equation (34)

$$e_P(k) = P_i(k) - P'_i(k) \quad (37)$$

is used to translate the effect to the battery by

$$E_{\text{shift,corr}}(k) = \begin{cases} E_{\text{shift}} + e_P T\, \eta_{\text{trans}}\, \eta_{\text{em}} \eta_{inv} & P_{\text{cycle}} < 0 \\ E_{\text{shift}}(k) + \frac{e_P(k)\, T}{\eta_{\text{trans}}\, \eta_{\text{em}} \eta_{\text{inv}}} & P_{\text{cycle}} \geq 0 \end{cases} \quad (38)$$

where the time grid spacing is $T = 1\text{s}$. The resulting torque is corrected in the same way as the energy change in (38) by

$$T_{\text{em,corr}} = T_{\text{em}} + e_P \frac{\eta_{\text{trans}}}{\frac{g_r v}{r_{\text{wheel}}}} \quad P_{\text{cycle}} < 0 \quad . \quad (39)$$

The consideration of these correction terms leads to results close to standard DP (Fig. 6 and Fig. 7) but comes along with significantly reduced computation costs.

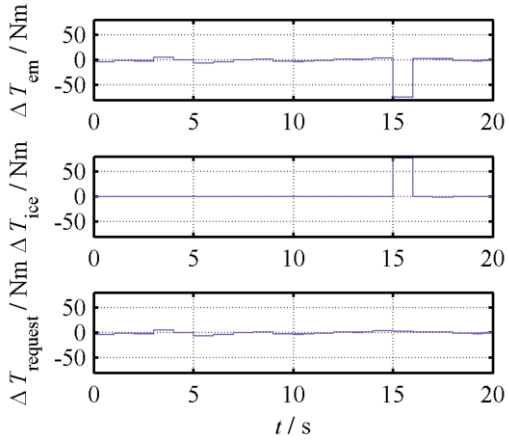

Fig. 5. Difference of torques T_{em} and T_{ice} and the overall difference $\Delta T_{\text{request}}$

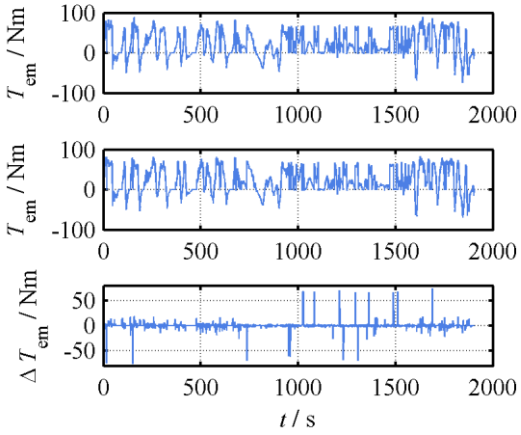

Fig. 6. Optimal electric motor torque T_{em} trajectory calculated by standard DP (middle), lookup table based DP (above) and their difference (bottom)

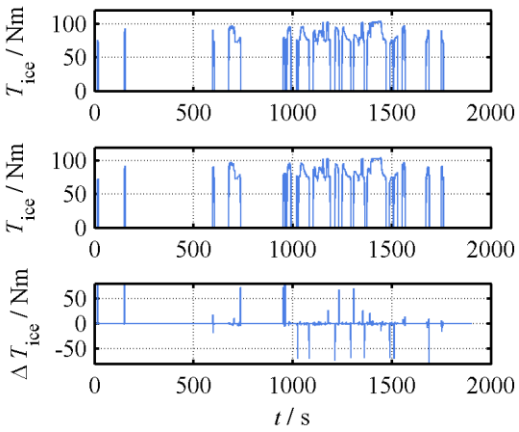

Fig. 7. Optimal electric motor torque T_{ice} trajectory calculated by standard DP (middle), lookup table based DP (above) and their difference (bottom)

4 Results

The EMS is simulated for the recorded real life cycle BCN-CTS employing CD mode. The obtained results are compared to the global optimal results calculated using standard DP. For both algorithms it is assumed that exact knowledge of the future trip is given in respect to speed and road grade. The comparison between the lookup tabled DP approach and the global optimum calculated by standard DP is done by applying the calculated optimal torque $T_{\mathrm{ice}}^{\mathrm{opt}}$, $T_{\mathrm{em}}^{\mathrm{opt}}$ and gear g^{opt} to the vehicle forward model. These results are used for the evaluation of the result. The driver model inside the vehicle forward model corrects differences in the torque distribution of the lookup table based DP by adjusting T_{em} with its PI controller. In that way it is assured that the comparison is done with the correct vehicle speed at every instance.

The remaining rounding error of the cycle power e_P despite the correction by (38) and (39) results in small differences of the costs at every time step. These differences of the cost function $J(k)$, (i.e. the fuel mass m_{fuel}) at particular time steps of the cycle between lookup table based DP and standard DP can lead to different decisions of the shortest path search algorithm. This behavior can be observed at the differences ΔT_{em} and ΔT_{ice} of the optimized torques T_{ice} and T_{em} (Fig. 6 bottom, Fig. 7 bottom). These shortest path decisions can be seen well when switching on the engine at different instances, resulting in peaks of the torque difference

$$\Delta T_{\mathrm{em}} = T_{\mathrm{em}}^{\mathrm{opt,LT-DP}} - T_{\mathrm{em}}^{\mathrm{opt,Std-DP}} \quad , \quad (40)$$

$T_{\mathrm{em}}^{\mathrm{opt,LT-DP}}$ being the results of lookup tabled based DP. At second 15 (Fig. 5) the lookup table based DP leaves the engine switched off, while it is switched on by standard DP. However, this behavior does not hamper the overall results, as the sum T_{request} of both torques does not show these peaks (Fig. 6, bottom).

Due to the grid spacing of the wheel power P_{wheel} of 1kW, the rounding error e_p is always smaller than 0.5kJ. This error e_p of the wheel power affects at lower vehicle speed the torque difference $\Delta T_{\mathrm{request}}$ more than at higher vehicle speed (Fig. 8). Between second 1450-1500 the vehicle speed is between 119.2 and 127.4km/h and the resulting torque difference $|\Delta T_{\mathrm{request}}|$ is smaller than 2Nm. For the part with smaller vehicle speed has a short increase to values $|\Delta T_{\mathrm{request}}| < 12.6\mathrm{Nm}$ and changes from second 212 at values $|\Delta T_{\mathrm{request}}| < 5\mathrm{Nm}$. Due to the changing nature of the sign of the error the overall performance is only slightly affected (Fig. 9).

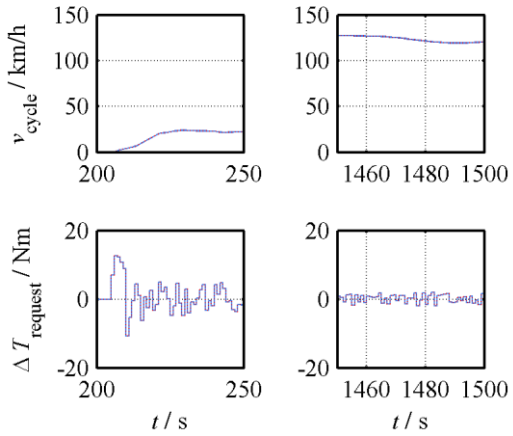

Fig. 8. Torque differences during seconds 200-250 and 1450-1500. The cycle speed in the second time window is higher than in the first one, thus the power rounding error e_p due to the lookup table leads to smaller torque differences.

By the use of lookup tables for the DP algorithm, a drastic reduction of calculation time is achieved. Table III shows an improvement of computation time by a factor of around 50 for the lookup table based DP. A further reduction of the computation cost can be achieved by the reduction of the prediction horizon [20].

Table III: Calculation time. The times refer to a calculation on Intel i3 at 1.8GHz. For the lookup tables based values the calculation of the lookup tables is not included.

Standard DP	44732s
Lookup table based DP	808s
Computation time improvement factor	55

Comparing energy managements for PHEV is not straightforward if the final SOC value at the end of the driving cycle is not the same, as it is here the case. As the PHEV consumes both fuel and electric energy, the total energy consumption E_{total} and the resulting CO_2 emission are compared by

$$E_{\text{total}} = E_{\text{electric}} + E_{\text{fuel}} = \Delta\text{SOC} \cdot E_{\text{battery}} + m_{\text{fuel}} \cdot H_i \quad (41)$$

where H_i the higher heating value of the fuel used by the engine. For the CO_2 emission the consumed fuel and the CO_2 generation resulting from the electricity production is considered (10), using data of the average emission of the electricity production in the EU in 2009 (appr. 396/kWh [21]). The additional CO_2 output by the transport and the losses by charging the battery are neglected. Therefore, the resulting equation is:

$$m_{\text{CO2}} = m_{\text{CO2,electric}} + m_{\text{CO2,fuel}} = \frac{110\text{g}}{\text{MJ}} E_{\text{electric}} + \frac{31.733\text{g}}{kg} m_{\text{fuel}} \quad (42)$$

The difference of the calculated carbon dioxide emission per km is 0.08% (Table IV). The resulting SOC curve during the cycle of for the lookup table based DP close to the results achieved with standard DP (Fig. 9). The resulting SOC is at every moment close to the global optimum, reaching a final SOC of 0.299. The difference of the results of the standard DP applied to the forward model (compare Table IV, column 1, 3) is caused by the discretization of the change of the energy levels at every step and the discrete time steps (Fig. 3) and can only be reduced by finer grid spacing. However, the possibly higher exactness (now having an error of only 0.1% for the overall used electric energy) would not compensate the increasing computation cost.

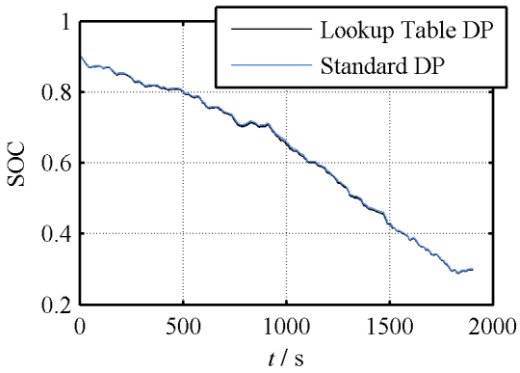

Fig. 9. Optimal SOC applying the results from standard DP (light blue) and from lookup table based DP (black)

Table IV: Simulation results of consumption

	Standard DP	Lookup Table DP	Error / %
$\text{SOC}_{\text{final}}$	0.3007	0.2988	-
V_{fuel} / l/100km	3.35	3.35	0.03
$E_{\text{battery}}/\frac{\text{kWh}}{\text{100km}}$	7.25	7.26	0.32
E_{total} / MJ	42.715	42.792	0.18
m_{CO2} / g/km	109.4	109.5	0.08

5 Conclusion

The proposed algorithm yields a significant acceleration of DP if used for EMS of a (P)HEV. Necessary for the speed gain is the repeated use of the algorithm for the same vehicle type. In this case the speed gain of the computation compared to standard DP is approximately by the factor of 50. This speed gain brings its application in real time energy managements closer. If used in combination with techniques for a reduced prediction horizon, the calculation time can be further reduced. The results obtained are close to the results obtained by standard DP with a deviation of optimal fuel consumption of less than 0.03% and of the total energy of 0.18%. It is expected that the algorithm will show a similar performance in other driving cycles. The fact that the computation cost of the proposed energy management is not affected by the complexity of the vehicle model, allows the use of more exact losses model of electric motor, combustion engine, converter and transmission applying loss tables.

Acknowledgments

This work is part of the project VERDE. VERDE is a CENIT project funded by the Ministry of Economy and Competitiveness of the Government

of Spain. It is led by SEAT, coordinated by CTM Centre Tecnològic and integrated by the following companies: AIA, Cegasa, Circutor, Cobra, Endesa, Ficosa, Green Power, Iberdrola, Infranor, Lear, Mapro, Red Eléctrica España, Siemens, Rovalma and Tècnicas Reunidas. And Research Institutes: AICIA, ASCAMM, CIDETEC, CIRCE, CNM del CSIC, CTM Centre Tecnològic, IIC, IIT de la Universidad Pontificie de Comillas, IREC, Leitat, Tecnalia, Universitat Politècnica Catalunya (UPC) and Universidad Carlos III.

References

[1] J. Gonder and T. Markel, "Energy management strategies for plug-in hybrid electric vehicles," *Energy*, vol. 1, p. 0290, 2007.

[2] J. J. Valera García, "Control y gestión inteligente del sistema de propulsión en los vehículos eléctricos de autonomía extendida_," Universidad del País Vasco, Spain.

[3] S. G. Wirasingha and A. Emadi, "Classification and Review of Control Strategies for Plug-In Hybrid Electric Vehicles," *Ieee Trans. Veh. Technol.*, vol. 60, no. 1, pp. 111–122, 2011.

[4] S. Barsali, C. Miulli, and A. Possenti, "A control strategy to minimize fuel consumption of series hybrid electric vehicles," *Ieee Trans. Energy Convers.*, vol. 19, no. 1, pp. 187–195, 2004.

[5] X. Li, J. Li, L. Xu, and M. Ouyang, "Power management and economic estimation of fuel cell hybrid vehicle using fuzzy logic," in *IEEE Vehicle Power and Propulsion Conference, 2009. VPPC '09*, 2009, pp. 1749–1754.

[6] C.-Y. Li and G.-P. Liu, "Optimal fuzzy power control and management of fuel cell/battery hybrid vehicles," *J. Power Sources*, vol. 192, no. 2, pp. 525–533, 2009.

[7] N. Kim, S. Cha, and H. Peng, "Optimal Control of Hybrid Electric Vehicles Based on Pontryagin's Minimum Principle," *Ieee Trans. Control Syst. Technol.*, vol. 19, no. 5, pp. 1279–1287, 2011.

[8] S. Kermani, S. Delprat, T. M. Guerra, R. Trigui, and B. Jeanneret, "Predictive energy management for hybrid vehicle," *Control Eng. Pr.*, vol. 20, no. 4, pp. 408–420, Apr. 2012.

[9] S. Delprat, J. Lauber, T. M. Guerra, and J. Rimaux, "Control of a parallel hybrid powertrain: optimal control," *Veh. Technol. Ieee Trans.*, vol. 53, no. 3, pp. 872–881, 2004.

[10] S. Stockar, V. Marano, M. Canova, G. Rizzoni, and L. Guzzella, "Energy-Optimal Control of Plug-in Hybrid Electric Vehicles for Real-World Driving Cycles," *Ieee Trans. Veh. Technol.*, vol. 60, no. 7, pp. 2949–2962, Sep. 2011.

[11] Q. Gong, Y. Li, and Z. R. Peng, "Trip-based optimal power management of plug-in hybrid electric vehicles," *Veh. Technol. Ieee Trans.*, vol. 57, no. 6, pp. 3393–3401, 2008.

[12] V. Ngo, T. Hofman, M. Steinbuch, and A. Serrarens, "Optimal Control of the Gearshift Command for Hybrid Electric Vehicles," *Ieee Trans. Veh. Technol.*, vol. 61, no. 8, pp. 3531 –3543, Oct. 2012.

[13] P. Thounthong, S. Raël, and B. Davat, "Energy management of fuel cell/battery/supercapacitor hybrid power source for vehicle applications," *J. Power Sources*, vol. 193, no. 1, pp. 376–385, 2009.

[14] M.-J. Kim and H. Peng, "Power management and design optimization of fuel cell/battery hybrid vehicles," *J. Power Sources*, vol. 165, no. 2, pp. 819–832, 2007.

[15] D. Ambühl and L. Guzzella, "Predictive reference signal generator for hybrid electric vehicles," *Veh. Technol. Ieee Trans.*, vol. 58, no. 9, pp. 4730–4740, 2009.

[16] G. Rizzoni, L. Guzzella, and B. M. Baumann, "Unified modeling of hybrid electric vehicle drivetrains," *Ieeeasme Trans. Mechatronics*, vol. 4, no. 3, pp. 246 –257, Sep. 1999.

[17] R. E. Bellman, *Dynamic Programming*. Princeton, NJ: Princeton University Press, 1957.

[18] D. P. Bertsekas, *Dynamic programming and optimal control*, vol. 1. Athena Scientific Belmont, MA, 1995.

[19] M. Stiegeler, "Entwurf einer vorausschauenden Betriebsstrategie für parallele hybride Antriebsstränge," Universität Ulm. Fakultät für Ingenieurwissenschaften und Informatik, 2008.

[20] B. Bader, O. Torres, G. Lux, and J. L. Romeral, "Influence of the Prediction Horizon length of a PHEV Energy Management on Fuel consumption," presented at the EVS 26, Los Angeles, 2012.

[21] "European Environment Agency (EEA) - Data Viewer," *CO2 intensity of heat and electricity generation in 2009*. [Online]. Available: http://www.eea.europa.eu/data-and-maps/figures/co2-electricity-g-per-kwh. [Accessed: 23-May-2013].

Authors

Benjamin Bader received his degree in Electrical Engineering from the Technical University of Aachen (RWTH), Germany in 2009. Since 2010 he is Ph.D. student at the MCIA research group of the Technical University of Catalonia (UPC) working in the public research project VERDE on hybrid vehicles with SEAT. He is working on modelling and energy management of HEV and HIL simulation.

Oriol Torres received the Telecommunication Engineering degree from the Technical University of Catalonia (UPC) in 2010. Since 2010 is doing his Ph.D. degree in Electronics from the Technical University of Catalonia (UPC). His researches are focused on hybrid powertrain optimizations, modelling, simulation, and hardware in the loop (HIL) tests.

Juan Antonio Ortega (M'94) received the M.S. Telecommunication Engineer and Ph.D. degrees in Electronics from the Technical University of Catalonia (UPC) in 1994 and 1997, respectively. Since 2001 he belongs to the Motion Control and Industrial Applications research group working in the area of Motor Current Signature Analysis. His current R&D areas include: Motor diagnosis, Signal acquisition, Smart sensors, Embedded systems and Remote Labs.

Gerhard Lux received his Electrical Engineering degree in 2002 and his Ph.D. in Mechanical Engineering in 2008, both from the Vienna University of Technology, Austria. Since 2009 he is working at the SEAT Technical Centre, Spain, where he currently leads the hybrid and electric powertrain development.

Luis Romeral (M'98) received the Electrical Engineering degree and the Ph.D. degree from the Technical University of Catalonia (UPC) in 1985 and 1995 respectively. His research interests include electric machines, power electronics converters and modulation strategies, variable-speed drive systems, fault detection and motor diagnosis, and microprocessor-based real-time control algorithms. Dr. Romeral belongs to the Motion and Industrial Control Group (MCIA) at the UPC